

Phases and collective modes of a hardcore Bose-Fermi mixture in an optical lattice

S. Sinha¹ and K. Sengupta²

¹*Indian Institute of Science Education Research, HC Block, Sector III, Salt Lake, Kolkata 700106, India*

²*Department of Theoretical Physics, Indian Association for the Cultivation of Sciences, Jadavpur, Kolkata 700032, India and TCMP Division, Saha Institute of Nuclear Physics, 1/AF Bidhannagar, Kolkata 700064, India*

(Received 8 December 2008; revised manuscript received 14 February 2009; published 24 March 2009)

We obtain the phase diagram of a Bose-Fermi mixture of hardcore spinless bosons and spin-polarized fermions with nearest-neighbor intraspecies interaction and on-site interspecies repulsion in an optical lattice at half filling using a slave-boson mean-field theory. We show that such a system can have four possible phases which are (a) supersolid bosons coexisting with fermions in the Mott state, (b) Mott state of bosons coexisting with fermions in a metallic or charge-density wave state, (c) a metallic fermionic state coexisting with superfluid phase of bosons, and (d) Mott insulating state of fermions and bosons. We chart out the phase diagram of the system and provide analytical expressions for the phase boundaries within mean-field theory. We demonstrate that the transitions between these phases are generically first order with the exception of that between the supersolid and the Mott states which, within mean-field theory, is a continuous quantum phase transition. We also obtain the low-energy collective excitations of the system in these phases. Finally, we study the particle-hole excitations in the Mott insulating phase and use it to determine the dynamical critical exponent z for the supersolid-Mott insulator transition. We discuss experiments which can test our theory.

DOI: [10.1103/PhysRevB.79.115124](https://doi.org/10.1103/PhysRevB.79.115124)

PACS number(s): 67.60.Fp, 64.70.Tg, 73.22.Gk, 73.22.Lp

I. INTRODUCTION

Recent experiments on ultracold trapped atomic gases have opened a new window onto the phases of quantum matter.¹ A gas of bosonic atoms in an optical or magnetic trap has been reversibly tuned between superfluid (SF) and insulating ground states by varying the strength of a periodic potential produced by standing optical waves.¹ This transition has been explained on the basis of the Bose-Hubbard model with on-site repulsive interactions and hopping between nearest neighboring sites of the lattice.^{2,3} Further, theoretical studies of bosonic atoms with spin and/or pseudospin have also been undertaken.^{4,5} These studies have revealed a variety of interesting Mott¹ and supersolid⁶ phases and superfluid-insulator transitions³ in these systems. On the fermionic side, the experimental studies have mainly concentrated on the observation of paired superfluid states⁷ and the BCS-BEC crossover in such systems near a Feshbach resonance.⁸ More recently, it has been possible to generate mixtures of fermionic and bosonic atoms in a trap.⁹ Several theoretical studies followed soon, which established such Bose-Fermi mixtures to be interesting physical systems in their own right,^{10,11} exhibiting exciting Mott phases in the presence of an optical lattice.

Many of the earlier studies of Bose-Fermi mixtures have been restricted to one-dimensional (1D) systems¹² or have concentrated on regimes where the coupling between bosons and fermions are weak.¹³ The existence of a supersolid (SS) phase in these system in such a weak-coupling regime has also been predicted.¹⁴ Other works^{10,11} which have looked at the strong-coupling regime have restricted themselves to integer filling factors of bosons and fermions (per spin) and have therefore not addressed the phenomenon of translational symmetry breaking and possible associated SS phases in the strongly interacting regimes of these systems. More recently, however, Titvinidze *et al.*¹⁵ studied a mixture of

spinless softcore bosons with an on-site interaction U and spin-polarized noninteracting fermions at half-filling in a three-dimensional (3D) optical lattice using dynamical mean-field theory (DMFT). Several interesting phases, including a SS phase of bosons and charge-density wave (CDW) states of fermions, have been found in Ref. 15.

In this work, we study a mixture of hardcore spinless Bosons and spin-polarized interacting fermions in an optical lattice at half filling using a slave-boson mean-field technique. We concentrate on the case where both the bosons and the fermions have a nearest-neighbor density-density repulsive interaction in addition to the usual on-site interaction term between them. We provide an analytical, albeit mean-field, phase diagram for the system and demonstrate that the ground state of such a system consists of four distinct phases, namely, (a) a Mott insulating (MI) phase where both fermions and bosons are localized at the lattice sites, (b) a metal +SF phase where the fermions are in a metallic phase with a gapless Fermi surface and the bosons are in a superfluid state, (c) a SS phase where the Bosons are in the SS state while the fermions are localized at the lattice site, and (d) a CDW+MI phase of coexisting fermions with weak density-wave order along with Mott insulating bosons. We show, within mean-field theory, that the transitions between these phases are generically first order with the exception of that between the SS and the MI phases which is a continuous quantum phase transition. We also obtain the low-energy collective modes in the metal+SF, CDW+MI, and SS phases and demonstrate that they have linear dispersions with definite group velocities. Further, in the MI phase which has no gapless modes, we find the dispersion of the gapped particle-hole excitations and use it to determine the dynamical critical exponent z for the continuous MI-SS transition. We also discuss realistic experiments which can test our theory.

The plan of rest of the paper is as follows. In Sec. II A, we develop a slave-Boson mean-field theory for the system. This is followed by Sec. II B, where the mean-field phase

diagram is charted out. In Sec. III, we obtain the low-energy collective modes of the system in the metal+SF, CDW+MI, and SS phases. This is followed by Sec. IV where we discuss the gapped particle-hole excitations of the MI phase and use it to determine z for the SS-MI transition. We discuss relevant experiments which can test our theory and conclude in Sec. V

II. SLAVE-BOSON MEAN-FIELD THEORY

A. Mean-field equations

The Hamiltonian of the Bose-Fermi mixture in a d -dimensional hypercubic lattice is described by the Hamiltonian

$$H = H_F + H_B + H_{FB}, \quad (1)$$

$$H_F = -t_F \sum_{\langle ij \rangle} c_i^\dagger c_j + V_F \sum_{\langle ij \rangle} n_i^F n_j^F, \quad (2)$$

$$H_B = -t_B \sum_{\langle ij \rangle} b_i^\dagger b_j + V_B \sum_{\langle ij \rangle} n_i^B n_j^B, \quad (3)$$

$$H_{FB} = U \sum_i n_i^F n_i^B, \quad (4)$$

where c_i (b_i) and $n_i^F = c_i^\dagger c_i$ ($n_i^B = b_i^\dagger b_i$) denote the annihilation and number operators for fermions (bosons) at site i , V_F (V_B) and t_F (t_B) denote the nearest-neighbor interaction strengths and hopping amplitudes for the fermions (bosons), respectively, U represents the amplitude for on-site interaction between the fermions and the bosons, and $\sum_{\langle ij \rangle}$ represents sum over nearest neighbor ij pairs on the lattice. In what follows, we shall study the Hamiltonian at half filling. We note at the outset that this constraint of half filling implies $n_i^F, n_i^B \leq 1$ at each site. An inspection of the Hamiltonian [Eq. (1)] shows that the ground state of the system shall be a Mott state for both bosons and fermions when $V_B, V_F \gg t_F, t_B$ whereas in the opposite limit, it will be a mixture of superfluid bosons and metallic fermions. Our subsequent analysis reveals two additional phases of the system as indicated in Sec. I.

To obtain an analytical understanding of the phases of these model, we first introduce a slave-boson representation for the fermions, $c_i = a_i d_i$, where a_i denotes annihilation operator for the slave bosons and d_i represents the annihilation operator for pseudofermions. We note that in this representation, the anticommutation relation for the fermionic operator $[c_i^\dagger c_j]_{\pm} = \delta_{ij}$, where δ_{ij} denotes the Kronecker delta, enforces the constraint $n_i^d = n_i^a$ on each site. In terms of these slave bosons and pseudofermions, the Hamiltonians H_F and H_{FB} in Eqs. (2) and (4) can be written as

$$H'_F = -t_F \sum_{\langle ij \rangle} d_i^\dagger a_i^\dagger a_j d_j + V_F \sum_{\langle ij \rangle} n_i^a n_j^a + \sum_i \lambda_i (n_i^a - n_i^d), \quad (5)$$

$$H'_{FB} = U \sum_i n_i^a n_i^B, \quad (6)$$

where we have implemented the constraint $n_i^d = n_i^a$ using Lagrange multipliers λ_i at each site and have used the fact

that $n_i^a = n_i^d = n_i^F \leq 1$ at each site i . We note that the Hamiltonian $H' = H_B + H'_F + H'_{FB}$ is exact and is completely equivalent to H [Eq. (1)].

To make further progress, we proceed with mean-field approximation of H' . To this end, we first decompose the quartic hopping term in Eq. (5) using

$$t_F \sum_{\langle ij \rangle} d_i^\dagger a_i^\dagger a_j d_j = t_1 \sum_{ij} a_i^\dagger a_j + t_2 \sum_{\langle ij \rangle} d_i^\dagger d_j - \frac{N t_2 t_1}{t_F}, \quad (7)$$

where N is the number of sites in the lattice and the hopping amplitudes t_1 and t_2 are given by

$$t_1 = \frac{t_F}{N} \sum_{\langle ij \rangle} \langle d_i^\dagger d_j \rangle_0, \quad t_2 = \frac{t_F}{N} \sum_{\langle ij \rangle} \langle a_i^\dagger a_j \rangle_0. \quad (8)$$

Here $\langle \dots \rangle_0$ denotes average with respect to the ground state of the system. Next, we use a mean-field approximation for the constraint term and approximate the Lagrange multiplier field $\lambda_i = \lambda_0 + \Delta(-1)^i$, where for sake of definiteness, we take $i = i_1 + i_2 + \dots + i_d$ to be even for A sublattice sites. Such an ansatz for λ_i is motivated by the fact that it is the simplest mean-field ansatz that preserves the basic symmetries of the problem and, at the same time, allows for translational symmetry breaking in the pseudofermion sector. With these approximations, the mean-field Hamiltonian for the system can be written as

$$\begin{aligned} H_{MF} = & -t_2 \sum_{\langle ij \rangle} d_i^\dagger d_j + \Delta \sum_i (-1)^i (n_i^a - n_i^d) \\ & + \sum_{\langle ij \rangle} (V_F n_i^a n_j^a - t_1 a_i^\dagger a_j) + \sum_i U n_i^a n_i^B \\ & + \sum_{\langle ij \rangle} (V_B n_i^B n_j^B - t_B b_i^\dagger b_j) + \frac{N t_2 t_1}{t_F}. \end{aligned} \quad (9)$$

In writing Eq. (9), we have ignored the term $\lambda_0 \sum_i (n_i^d - n_i^a)$ since it merely renormalizes the chemical potential of the fermions and thus behave like a constant as long as we restrict ourselves to half filling.

To obtain the ground-state energy corresponding to this mean-field Hamiltonian, we now use a variational ansatz for the ground-state wave function

$$|\Psi\rangle_0 = \prod_{i \in A} |\psi_A\rangle \otimes \prod_{i \in B} |\psi_B\rangle \otimes |FS\rangle,$$

$$|\psi_A\rangle = [\cos(\theta) |n^B = 0\rangle + \sin(\theta) |n^B = 1\rangle] \otimes [\cos(\gamma) |n^a = 0\rangle + \sin(\gamma) |n^a = 1\rangle],$$

$$|\psi_B\rangle = [\cos(\theta) |n^B = 1\rangle + \sin(\theta) |n^B = 0\rangle] \otimes [\cos(\gamma) |n^a = 1\rangle + \sin(\gamma) |n^a = 0\rangle],$$

$$|FS\rangle = \prod_{\mathbf{k}} \theta(|\mathbf{k}| - k_F) d_{\mathbf{k}}^\dagger |0\rangle, \quad (10)$$

where k_F denotes the Fermi wave vector for the pseudofermions and θ and γ are variational parameters which has to be determined by minimizing the ground-state energy. Note that the variational wave function given by Eq. (10) has a two-

sublattice structure which allows for the possibility of translational symmetry broken phases. For the current system, where the fermions and the bosons both interact via nearest-neighbor density-density interaction terms, Eq. (10) is the simplest possible mean-field variational wave function which respects all the symmetries of the Hamiltonian. We would like to point out here that capturing the phases of a Bose-Fermi mixture with such interaction terms is beyond the scope of any single-site mean-field theory including single-site DMFT.

The variational mean-field energy $E_v = \langle \Psi | H_{\text{MF}} | \Psi \rangle$ of the system can now be easily obtained and is given by

$$\begin{aligned} \frac{E_v}{Nt_F} = & -\frac{d}{2}[Z' \sin^2(2\gamma) + Z \sin^2(2\theta)] \\ & + \frac{U'}{2}[\cos^2(\gamma)\cos^2(\theta) + \sin^2(\gamma)\sin^2(\theta)] \\ & - \frac{\Delta'}{2} \left(\cos(2\gamma) + \frac{2}{N} \langle \text{FS} | \sum_i (-1)^i d_i^\dagger d_i | \text{FS} \rangle \right) \\ Z' = & (t_1 - V_F)/t_F, \quad Z = (t_B - V_B)/t_F, \end{aligned} \quad (11)$$

where we have used $t_2/t_F = \sin^2(2\gamma)$, $\Delta' = \Delta/t_F$, and $U' = U/t_F$ and t_1/t_F has to be determined from Eq. (8). The corresponding mean-field equations which determine the ground-state values of the variational parameters are given by $\partial E_v / \partial \theta = \partial E_v / \partial \gamma = \partial E_v / \partial \Delta' = 0$ and yields

$$\begin{aligned} \sin(2\theta) \left[\frac{U'}{2} \cos(2\gamma) + 2Zd \cos(2\theta) \right] &= 0, \\ \sin(2\gamma) \left[\frac{U'}{2} \cos(2\theta) + 2Z'd \cos(2\gamma) - \Delta' \right] &= 0, \\ \cos(2\gamma) + \frac{2}{N} \langle \text{FS} | \sum_i (-1)^i d_i^\dagger d_i | \text{FS} \rangle &= 0. \end{aligned} \quad (12)$$

Next, we evaluate the effective hopping amplitude t_1 and $2/N \langle \text{FS} | \sum_i (-1)^i d_i^\dagger d_i | \text{FS} \rangle$. To this end, first, let us consider the pseudofermion Hamiltonian $\tilde{H} = -t_2 \sum_{\langle ij \rangle} d_i^\dagger d_j - \Delta \sum_i (-1)^i n_i^d$. The energy spectrum of \tilde{H} is given by $\pm E(\mathbf{k})$, where $E(\mathbf{k}) = \sqrt{\epsilon(\mathbf{k})^2 + \Delta^2}$, $\epsilon(\mathbf{k}) = -2t_2 \sum_{i=1, d} \cos(k_i a)$ is the energy dispersion of free fermions in a hypercubic lattice in d dimensions, and a is the lattice spacing which we shall, from now on, set to unity. The density of states (DOS) corresponding to these fermions are therefore given by

$$\begin{aligned} \rho(E) &= \rho_0(\sqrt{E^2 - \Delta^2}) \frac{\sqrt{E^2 - \Delta^2}}{E}, \\ \rho_0(\tilde{\epsilon}) &= \frac{1}{2t_2} \int \frac{d^d k}{(2\pi)^d} \delta \left[\tilde{\epsilon} - \sum_{i=1}^d \cos(k_i) \right], \end{aligned} \quad (13)$$

where ρ_0 denotes the DOS of free fermions with tight-binding dispersion on a hypercubic lattice, $\tilde{\epsilon} = \epsilon/2t_2$, and we have used the relation $\rho(E)dE = \rho_0(\epsilon)d\epsilon$. It is convenient to use Eq. (13) to express the expectation values over pseudo-

fermion ground states in Eqs. (8) and (12) and one obtains

$$\begin{aligned} \cos(2\gamma) &= -\tilde{\Delta} I_1(\tilde{\Delta}), \quad t_1 = t_2 I_2, \\ I_1(\tilde{\Delta}) &= \frac{\int_{-1}^0 \frac{1}{\sqrt{\tilde{\epsilon}^2 + \tilde{\Delta}^2}} \rho_0(\tilde{\epsilon}) d\tilde{\epsilon}}{\int_{-1}^0 \rho_0(\tilde{\epsilon}) d\tilde{\epsilon}}, \quad (14) \\ I_2 &= \frac{\int_{-1}^0 \tilde{\epsilon} \rho_0(\tilde{\epsilon}) d\tilde{\epsilon}}{\int_{-1}^0 \rho_0(\tilde{\epsilon}) d\tilde{\epsilon}}. \end{aligned} \quad (15)$$

Equations (12), (14), and (15) denote the complete set of mean-field equations which can be now solved to determine the mean-field phase diagram.

B. Phase diagram

Equations (12) and (14) can be easily solved numerically to obtain the mean-field phase diagram for the system. However, before resorting to numerics, we provide a qualitative discussion of the nature of the phases.

We find that Eqs. (12) and (14) yield four distinct solutions which correspond to four possible phases of the system. First, we find a MI phase with broken translational symmetry where both the fermions and the bosons are localized. Such a phase corresponds to the solution¹⁶

$$\theta = 0, \quad \gamma = \pi/2, \quad \tilde{\Delta} \rightarrow \infty. \quad (16)$$

Note that the divergence of $\tilde{\Delta}$ corresponds to $t_2 \rightarrow 0$ which in turn ensures that $\cos(2\gamma) = -1$. Such a MI state corresponds to a intertwined checkerboard density-wave pattern where the Fermions are localized in sublattice A [$n_i^a = \sin^2(\gamma) = n_i^d = 1$ for $i \in A$] and the Bosons are localized in sublattice B [$n_i^b = \cos^2(\theta) = 1$ for $i \in B$]. The mean-field energy of this state is $E_1 = 0$.

Second, we find a SS phase, where the Bosons are in a supersolid phase with coexisting density wave and superfluid order and the Fermions are localized in a Mott phase. Such a state corresponds to the solution

$$\cos(2\theta) = \frac{U'}{4Zd}, \quad \gamma = \pi/2, \quad \tilde{\Delta} \rightarrow \infty. \quad (17)$$

Such a state has $\langle b \rangle = \sin(2\theta)/2 \neq 0$ and $\langle (-1)^i b_i^\dagger b_i \rangle = -\cos(2\theta) \neq 0$ and thus corresponds to a SS phase for the bosons. Note that the realization of this state necessarily requires $U'/4Zd < 1$. For $U'/4Zd = 1$, $\theta = 0$ and we recover the MI state where $\langle b \rangle = 0$. The energy of the SS state is per site given by

$$E_2 = -\frac{Zdt_F}{2} \left(\frac{U'}{4Zd} - 1 \right)^2. \quad (18)$$

Third, we find the MI+CDW state where the fermions show weak density-wave oscillations whereas the Bosons are

localized in the MI state. This corresponds to the solution

$$\theta = 0, \quad \gamma = \gamma_0 \neq 0, \pi/2, \quad (19)$$

where γ_0 and Δ are to be determined from a numerical solution of the mean-field equations

$$\cos(2\gamma_0) = -\frac{U'}{4Z'd}(1 - 2\Delta/U) = -\tilde{\Delta}I_1(\tilde{\Delta}). \quad (20)$$

The energy of this state per site is given by

$$E_3 = \frac{U \cos^2(\gamma_0)}{2} \left(1 - \frac{4Z'd}{U'} \sin^2(\gamma_0) \right). \quad (21)$$

Finally, we find the state in which the superfluid Bosons coexist with metallic Fermions. This corresponds to the solution

$$\theta = \gamma = \pi/4 \quad \Delta = 0. \quad (22)$$

Note that such a phase has $\langle b \rangle = \sin(2\theta)/2 = 1$ and $\langle (-1)^i b_i^\dagger b_i \rangle = -\cos(2\theta) = 0$ so that the Bosons are in a uniform superfluid state. Also, $\Delta = 0$ and $\langle (-1)^i a_i^\dagger a_i \rangle = -\cos(2\gamma) = 0$ in this state indicating that the fermions are in a gapless uniform metallic state. The energy of this state per site is given by

$$E_4 = \frac{U}{4} \left[1 - \frac{2d}{U'}(Z + Z') \right]. \quad (23)$$

The phase boundaries corresponding to these phases can be analytically computed using Eqs. (18), (21), and (23), provided γ_0 and t_1 (which determines Z') are obtained from numerical solutions of Eqs. (20) and (8). For the MI phase to occur, we must have E_2, E_3 , and $E_4 \geq E_1 = 0$ which yields the conditions

$$\left(1 - \frac{2d}{U'}(Z + Z') \right) \geq 0, \quad Z \leq 0 \quad \text{and} \quad \frac{U'}{4|Z|d} \leq 1, \quad (24)$$

$$\frac{4Z'd}{U'} \sin^2(\gamma_0) \leq 1.$$

Note that the condition $U'/(4|Z|d) \leq 1$ which is necessary for the realization of the SS phase has to be simultaneously satisfied with the condition $Z \leq 0$ to make sure that the SS phase is actually a competing candidate to the MI state. The MI phase can indeed be realized in the parameter regime $Z \geq 0$ provided $U' > 4|Z|d$. The first condition $(Z + Z') \leq U'/2d$ shows that the MI phase is favored over the metal+SF phase for large U/d and predicts a linear phase boundary in the $U' - Z$ plane $U' = 2d(Z + Z')$ with a slope of $2d$ and intercept of $2dZ'$ between these two phases. Note that the MI phase always wins over the metal+SF phase if the nearest-neighbor interactions between the bosons and fermions are large compared to their hopping amplitudes making $Z + Z'$ negative. The final condition $\frac{4Z'd}{U'} \sin^2(\gamma_0) \leq 1$ indicates that the phase boundary between the MI and MI+CDW phases is independent of Z . The former phase is favored over the latter for larger U and smaller Z' .

Similarly for the SS phase to occur one needs $U'/(4|Z|d) < 1$ and $E_2 \leq E_1, E_3$, and E_4 which yield

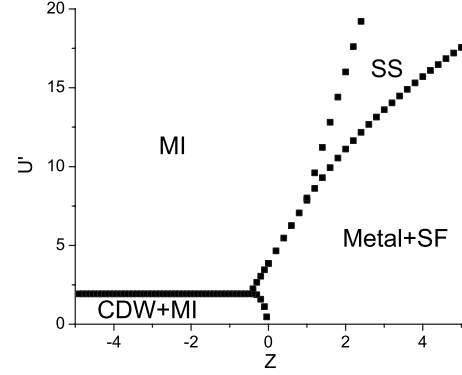


FIG. 1. Ground-state phase diagram as a function of Z and U' for noninteracting Fermions ($V_F=0$). The phase boundaries coincide with the analytical mean-field phase boundaries (see text for details).

$$\frac{U'}{Zd} \cos^2(\gamma_0) \left(\frac{4Z'd}{U'} \sin^2(\gamma_0) - 1 \right) \leq \left(\frac{U'}{4Zd} - 1 \right)^2, \quad (25)$$

$$Z \geq 0, \quad \frac{4Z'd}{U'} \sin^2(\gamma_0) \leq 1, \quad \frac{U'}{4\sqrt{ZZ'd}} \geq 1.$$

We note that the SS phase is favored when the nearest-neighbor interaction between the bosons are weak compared to their hopping amplitudes making Z positive and when U' is small enough so that $U'/(4|Z|d) < 1$. Also, from the conditions in Eq. (25) (obtained using $E_2 \leq E_4, E_1$), we note that for a given Z' and d , the boundary between the metal+SF and the SS phases is a parabola in the $U' - Z$ plane given by $U'^2 = 16ZZ'd^2$ while that between the SS and the MI state is a line given by $U' = 4Zd$.

Finally, the condition for occurrence of the metal+SF phase is given by $E_4 \leq E_1, E_2$, and E_3 , and is given by

$$\left(1 - \frac{2d}{U'}(Z + Z') \right) \leq 0, \quad \frac{U'}{4\sqrt{ZZ'd}} \geq 1 \quad \text{and} \quad \frac{U'}{4|Z|d} \leq 1, \quad (26)$$

$$\left(1 - \frac{2d}{U'}(Z + Z') \right) \leq 2 \cos^2(\gamma_0) \left(1 - \frac{4Z'd}{U'} \sin^2(\gamma_0) \right).$$

The last condition in Eq. (26) determines the phase boundary between the metal+SF and the MI+CDW phases which depends on value of γ_0 . However, numerically, we find that for $U \approx 0, \gamma_0 \approx \pi/4$, and in this regime, the phase boundary between these phases occurs at $Z \approx 0$ for all Z' and d . Note that strictly at $U=0$, the Fermionic state is metallic; however a CDW gap opens up in the Fermionic spectrum for an infinitesimal finite U' .

To verify the above-mentioned qualitative arguments and to find a precise phase diagram for the system, we numerically solve Eqs. (12), (14), and (15) for $d=2$ and for representative values $V_F/t_F=0, 0.5$. We plot the ground-state phase diagram as a function of Z and U' in Figs. 1 and 2. We find that the numerical results agree well with the qualitative arguments. Figures 1 and 2 indicate that the phase boundary

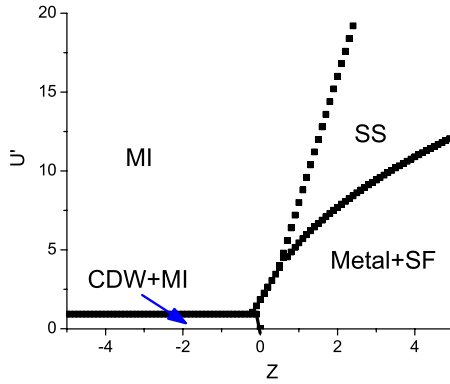


FIG. 2. (Color online) Same as in Fig. 1 but for $V_F/t_F=0.5$. The interaction between the Fermions favors the SS phase as can be seen by comparing Figs. 1 and 2.

between the CDW+MI and MI phases is independent of Z as noted earlier. The linear and the parabolic natures of the phase boundaries between the MI and SS phases and the SS and metal+SF phases, respectively, can also be easily verified from the figures and are in accordance with the qualitative discussion. We note that one of the effects of nearest-neighbor repulsion between the fermions is to enhance the SS phase which occupies a larger region of phase space in Fig. 2 ($V_F/t_F=0.5$) than in Fig. 1 ($V_F=0$). Such an interaction, for $Z \leq 0$, also favors the Mott phase over the CDW+MI phase as can also be seen from Figs. 1 and 2.

To determine the nature of transition between the different phases, we plot the ground-state values θ as a function of Z for $U'=10$ and $V_F/t_F=0.5$ in Fig. 3. Such a plot clearly shows that the transition between the metal+SF and the SS phases is, within the mean-field theory considered here, first order and is accompanied by a jump in the value of θ . In contrast, the SS-MI transition turns out to be continuous. A similar plot of ground-state values γ as a function of U' for $Z/t_F=-2$ and $V_F=0$, shown in Fig. 4, indicates that the transition between the CDW+MI and the MI phases is also discontinuous and is accompanied by a jump in the ground-state value of γ .

Next, we compare our phase diagram to that obtained from DMFT in Ref. 15. This can be done in the regime of

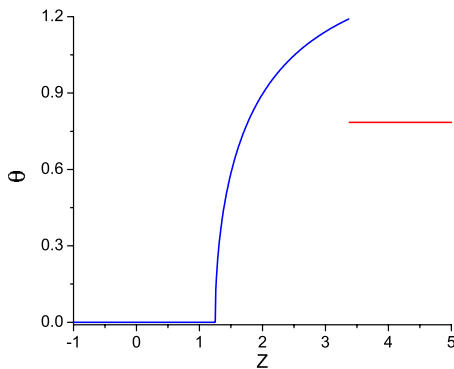


FIG. 3. (Color online) Variation of ground-state value of θ with Z for $U'=10$ and $V_F/t_F=0.5$. The discontinuity in θ at $Z=3.38$ indicates a first-order transition between the metal+SF and the SS phases. The transition between the SS and the MI phases is continuous.

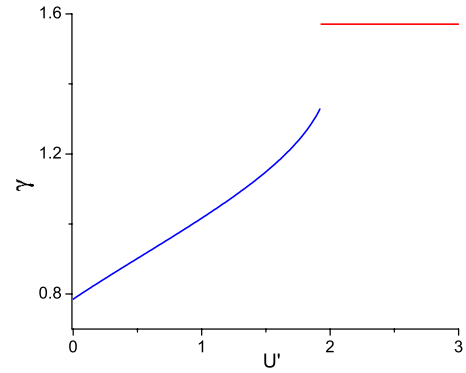


FIG. 4. (Color online) Variation of the ground-state value of γ with U' for $Z=-2$ and $V_F=0$. The discontinuity in γ at $U'=2$ indicates a first-order transition between the CDW+MI and the MI phases.

large positive Z (which corresponds to $V_B/t_B \rightarrow 0$) which was the case treated in Ref. 15. We find that the two phase diagrams qualitatively agree in the sense that both yield SS and MI phases in these limits. The difference lies in the fact that our mean-field predicts a second-order transition between the two phases whereas DMFT yields a narrow region of coexistence. This is presumably an effect of quantum fluctuation which is not captured within the mean-field theory. In addition, we also find a region of metal+SF phase at low U which was not seen in Ref. 15.

Finally, we would like to point out that the slave-boson mean-field phase diagram obtained above yields qualitatively correct phase diagram, but not a quantitatively correct one. This can be most clearly seen by noting that our Hamiltonian reduces to an effective Falicov-Kimball (FK) model¹⁷ in the limit $Z=t_B=V_B=V_F=0$. This is most easily seen by writing our starting Hamiltonian H [Eq. (1)] for $t_B=V_B=V_F=0$,

$$H_{\text{FK}} = -t_F \sum_{\langle ij \rangle} c_i^\dagger c_j + U \sum_i c_i^\dagger c_i n_i^B. \quad (27)$$

At half filling the Bosons are localized in the B sublattice so that $n_i^B = [1 - (-1)^i]/2$. Thus the Fermions have a CDW instability even for an infinitesimal U due to nesting for half filling on a square lattice. Consequently, the FK model at half filling is insulating for any infinitesimal U , as known from several earlier studies.¹⁸ Such a CDW instability, which can be easily captured by weak-coupling mean-field theory, is not straightforward to obtain in our strong-coupling slave-boson mean-field approach which predicts a finite critical U for the transition from metal+SF to the MI phase. Note however that the slave-boson mean-field theory does predict a CDW+MI state for weak U , but for small negative Z , as can be seen from Fig. 1. This indicates that the phase diagram obtained has qualitatively, but not quantitatively, correct features.

III. COLLECTIVE MODES

The phases of the Bose-Fermi mixture discussed in Sec. II allows for two types of excitations. The first type is the low-energy gapless collective modes that are present in the

metal+SF, CDW+MI, and SS phases of the system. These are the gapless Goldstone modes corresponding to the boson and the slave-boson fields. For all of these modes, the pseudofermion sector remains gapped and does not contribute to their dispersion. The gapped modes correspond to particle-hole excitations in the CDW+MI, SS, and Mott states. In this section, we concentrate on the gapless collective modes in the CDW+MI, SS, and metal+SF phases.

To obtain the dispersion, we first consider a time-dependent variational wave function

$$|\Psi_d(t)\rangle_0 = [\cos(\theta_i)|n_i^B = 0\rangle + \sin(\theta_i)e^{-i\chi_i}|n_i^B = 1\rangle] \otimes [\cos(\gamma_i)|n_i^F = 0\rangle + \sin(\gamma_i)e^{-i\phi_i}|n_i^F = 1\rangle], \quad (28)$$

where θ_i , χ_i , γ_i , and ϕ_i are space-time-dependent fields. Note that in the static limit, the ground state of the system corresponds to $\theta_i = \theta_0 = \theta_0(\pi/2 - \theta_0)$ and $\gamma_i = \gamma_0 = \gamma_0(\pi/2 - \gamma_0)$ for $i \in A(B)$ sites, and $\chi_i = \phi_i = 0$, so that $|\Psi_d(t)\rangle$ reduces to $|\Psi\rangle$.

The Lagrangian $\mathcal{L} = \sum_i \langle \Psi_d(t) | i \partial_t - H' + \mu_B \sum_i n_i^B + \mu_F \sum_i n_i^F | \Psi_d \rangle$ can now be computed using the variational wave function and one obtains

$$\begin{aligned} \mathcal{L} = & \sum_i [\partial_t \chi_i \sin^2(\theta_i) + \partial_t \phi_i \sin^2(\gamma_i) - U \sin^2(\theta_i) \sin^2(\gamma_i)] \\ & + \sum_{\langle ij \rangle} \left[\frac{1}{4} (t_B \sin(2\theta_i) \sin(2\theta_j) \cos(\chi_i - \chi_j) \right. \\ & + t_1 \sin(2\gamma_i) \sin(2\gamma_j) \cos(\phi_i - \phi_j) \\ & \left. - \{V_F \sin^2(\gamma_i) \sin^2(\gamma_j) + V_B \sin^2(\theta_i) \sin^2(\theta_j)\} \right] \\ & + \sum_i [\Delta \{-\sin^2(\gamma_i) (-1)^i + \langle n_i^F \rangle\} + \mu_B \sin^2(\theta_i) \\ & + \mu_F \sin^2(\gamma_i)], \quad (29) \end{aligned}$$

where $\langle n_i^F \rangle = \langle FS | (-1)^i d_i^\dagger d_i | FS \rangle / N$ is the fermion number density different on A and B sublattices and all time dependence of the fields are kept implicit for the sake of clarity. To obtain the collective modes, we now write $\theta_i(t) = \theta_0 + \delta\theta_i(t)$ and $\gamma_i(t) = \gamma_0 + \delta\gamma_i(t)$ and expand the Lagrangian to quadratic order in $\delta\theta_i(t)$, $\delta\gamma_i(t)$, $\phi_i(t)$, and $\chi_i(t)$. Then a variation of this Lagrangian with respect to $\delta\theta_i(t)$, $\delta\gamma_i(t)$, $\phi_i(t)$, and $\chi_i(t)$ and consequent adjustment of values of the parameters μ_B and μ_F following Ref. 19 yield the equations for the low-energy collective modes (we set $\hbar = 1$ from now on)

$$\partial_t \delta\gamma_{\mathbf{k}} + t_1 d \sin(2\gamma_0) [1 - c(\mathbf{k})] \phi_{\mathbf{k}} = 0, \quad (30)$$

$$\partial_t \phi_{\mathbf{k}} - \alpha_1(\mathbf{k}) \delta\gamma_{\mathbf{k}} - U \sin(2\theta_0) \delta\theta_{\mathbf{k}} = 0, \quad (31)$$

$$\partial_t \delta\theta_{\mathbf{k}} + t_B d \sin(2\theta_0) [1 - c(\mathbf{k})] \chi_{\mathbf{k}} = 0, \quad (32)$$

$$\partial_t \chi_{\mathbf{k}} - \alpha_2(\mathbf{k}) \delta\theta_{\mathbf{k}} - U \sin(2\gamma_0) \delta\gamma_{\mathbf{k}} = 0, \quad (33)$$

where we have taken the Fourier transform of all the fields, $c(\mathbf{k}) = \sum_{j=1,d} \cos(k_j) / d$, and α_1 and α_2 are given by

$$\alpha_1(\mathbf{k}) = \frac{4t_1 d}{\sin(2\gamma_0)} \left[1 + c(\mathbf{k}) \left(\frac{V_F}{t_1} \sin^2(2\gamma_0) + \cos^2(2\gamma_0) \right) \right],$$

$$\alpha_2(\mathbf{k}) = \frac{4t_B d}{\sin(2\theta_0)} \left[1 + c(\mathbf{k}) \left(\frac{V_B}{t_B} \sin^2(2\theta_0) + \cos^2(2\theta_0) \right) \right]. \quad (34)$$

It is important to note that Eqs. (30) and (31) hold when $\gamma_0 \neq 0$ and $\pi/2$ while Eqs. (32) and (33) hold when $\theta_0 \neq 0$ and $\pi/2$. Thus none of these equations are valid in the MI phase which does not support any low-energy collective modes. The gapped modes of the MI phases will be obtained in Sec. IV.

In the SS phase where $\cos(2\theta_0) = U' / (4Zd) \neq 0, 1$ and $\gamma_0 = \pi/2$, the collective mode corresponds to the low-energy excitations of the bosons and is given by Eqs. (32) and (33). A simple set of standard manipulations of these equations yields the dispersion of the collective modes $\omega^2 = 2v_1^2(\mathbf{k}) [1 - c(\mathbf{k})]$, where

$$v_1^2(\mathbf{k}) = t_B d \sin(2\theta_0) \alpha_2(\mathbf{k}) / 2. \quad (35)$$

Note that for low momentum, we get a gapless linearly dispersing collective mode with velocity $v_{ss} = v_1(\mathbf{k} = \mathbf{0})$. Similarly for the MI+CDW phase, where $\theta_0 = 0$ and $\gamma = \gamma_0$, the collective mode corresponds to the low-energy excitations of the pseudobosons and can be obtained by solving Eqs. (30) and (31). Since the pseudofermion sector is always gapped in this phase ($\Delta \neq 0$), the collective mode here corresponds to the density-wave mode of the real fermions. These modes have linear dispersion $\omega^2 = 2v_2^2(\mathbf{k}) [1 - c(\mathbf{k})]$, where

$$v_2^2(\mathbf{k}) = t_1 d \sin(2\gamma_0) \alpha_1(\mathbf{k}) / 2. \quad (36)$$

Thus for low momenta, we again get a gapless linearly dispersing collective mode with velocity $v_{CDW} = v_2(\mathbf{k} = \mathbf{0})$.

Finally for the metal+SS phase, all the Eqs. (30)–(33) hold and they need to be solved simultaneously. In this phase since $\gamma_0 = \theta_0 = \pi/4$, we find that $\alpha_1(\mathbf{k}) = 4t_1 d [1 + c(\mathbf{k}) V_F / t_1]$ and $\alpha_2(\mathbf{k}) = 4t_B d [1 + c(\mathbf{k}) V_B / t_B]$. Solving these equations, one finds two collective modes with linear dispersions $\omega_{\pm}^2 = 2v_{\pm}^2(\mathbf{k}) [1 - c(\mathbf{k})]$, where $v_{\pm}(\mathbf{k})$ are given by

$$\begin{aligned} v_{\pm}^2(\mathbf{k}) = & \frac{1}{4} \left[[\alpha_1(\mathbf{k}) t_1 d + \alpha_2(\mathbf{k}) t_B d] \right. \\ & \left. \pm \sqrt{[\alpha_1(\mathbf{k}) t_1 d - \alpha_2(\mathbf{k}) t_B d]^2 + 16(U t_B t_1 d)^2} \right]. \quad (37) \end{aligned}$$

These collective modes result from the hybridization of the Bogoliubov modes of the bosons and the density-wave modes for the metallic fermions. This fact can be easily checked by putting $U = 0$ in Eq. (37) by which one can retrieve these modes with velocities $v_B^2(\mathbf{k}) = \alpha_2(\mathbf{k}) t_B d / 2$ for the bosons and $v_F^2(\mathbf{k}) = \alpha_1(\mathbf{k}) t_1 d / 2$ for the fermions. As U' increases, the hybridization between these modes becomes stronger until the velocity $v_-(\mathbf{k} = \pi)$ touches zero at $U' = 4\sqrt{|Z'Z|}d$ which is precisely the condition for the metal +SF phase to become unstable to the SS phase.

IV. GAPPED MODES IN THE MI PHASE

The MI phase, in contrast to the other three phases of the system, does not support a gapless mode. The lowest-lying

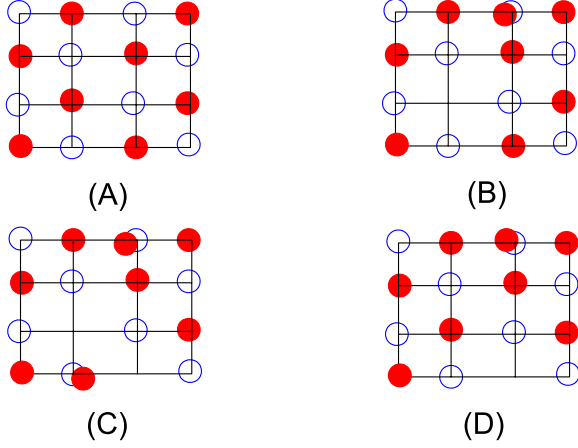


FIG. 5. (Color online) Cartoon representation of the MI state. (A) The Mott state at half filling. The red filled circles represent Bosons and the empty blue circles indicate Fermions. (B) A particle and a hole excitation which are not nearest neighbors. (C) An intermediate virtual high-energy state which assists hopping of holes. (D) A state where the hole has hopped to the next-neighbor site. This state is identical in energy to the state (B).

excitations of such a state with conserved number density are particle-hole excitations. Such excitations are of two types. The first type, shown in second panel of Fig. 5, involves particle and hole excitations that are spatially well separated while the second type, shown in second panel of Fig. 6, involves particle and hole excitations in nearest-neighbor sites which form a dipole. In what follows, we first compute the energies of both these excitations using perturbation theory up to second order in $t_{B/F}/V_{B/F}$ which are supposed to be small in the MI phase.

Such an energy estimate can be easily carried out by strong-coupling perturbation theory developed in Ref. 20 in the context of single species Bose-Hubbard model. The gen-

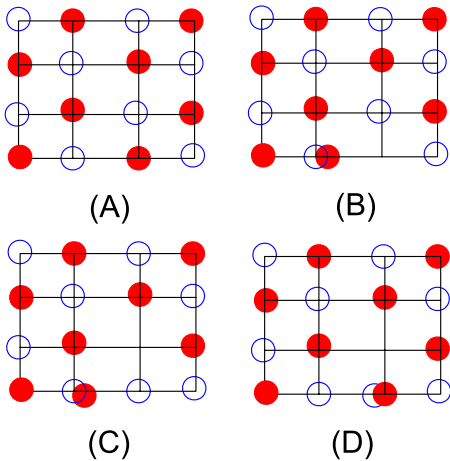


FIG. 6. (Color online) Cartoon representation of the MI state and the associated dipole excitations. All symbols are same as in Fig. 5. (A) The Mott state at half filling. (B) A dipole excitation over the Mott state. (C) An intermediate virtual high energy state which assists hopping of dipoles. (D) A state where the dipole has hopped to an adjacent link. This state is identical in energy to the state (B) when $V_F = V_B$.

eralization is largely trivial, except for one important detail. In the standard Bose-Hubbard model studied in Ref. 20, any particle/hole excitation could have lowering of energy via nearest-neighbor hopping which is $O(t/U)$ process. In contrast, as can be seen from Figs. 5 and 6, it is not possible for the particle-hole or dipole excitations to directly hop to the next site since such a direct hop always takes us out the low-energy manifold of states in the Mott limit. In particular, we note that any kinetic-energy gain of the particle-hole or dipole excitation must occur via hopping of the particle/hole to the second-neighbor sites and hence necessarily leads to $O(t^2/V^2)$ energy gain.

We first compute the excitation energy of the bosonic (fermionic) particle-hole pair when they are far apart. The on-site energy of creating such a pair is $E_{\text{on-site}}^{B/F} = 4dV_{B/F} + U$ while the energy lowering due to hopping of each of the particle and the hole is given by $E_{\text{hopping}}^{B/F} = -2d(2d-1)t_{B/F}^2/[2(2d-2)V_{B/F} + U]$. The energy of the Mott state to second order in perturbation theory is $E_{\text{MI}} = -d(t_B^2/[2(2d-1)V_B + U] + t_F^2/[2(2d-1)V_F + U])$ so that the excitation energy of the particle-hole pair is

$$E_{\text{p-h}}^{B/F} = 4dV_{B/F} + U - \frac{4d(2d-1)t_{B/F}^2}{2(2d-2)V_{B/F} + U} + \frac{dt_B^2}{2(2d-1)V_B + U} + \frac{dt_F^2}{2(2d-1)V_F + U}. \quad (38)$$

We note that in the limit of large d , where the mean-field results are expected to be accurate, we have

$$E_{\text{p-h}}^{B/F} \simeq 4dV_{B/F} + U - \frac{8d^2t_{B/F}^2}{4dV_{B/F} + U}. \quad (39)$$

The Mott state is destabilized in favor of the SS phase when $E_{\text{p-h}}^{B/F} = 0$.

Next, we compute the excitation energy of the bosonic/fermionic dipole state. We are going to do this in the limit of $V_F = V_B = V$. We note at the outset that once such a dipolar excitation is created, it remains stable, i.e., the hole cannot hop away arbitrarily far away from the particle. It can be easily verified from Fig. 6 that such hoppings generate higher-energy end states and take one out of the low-energy manifold of states.

The on-site energy cost for creating such an excitation is $E_{\text{on-site}} = 2(2d-1)V + U$ while the hopping process, shown schematically in Fig. 6, necessarily involves hopping of both fermions and bosons and leads to an energy gain of $E_{\text{hopping}}^d = t_B t_F / 2(2d-1)V$. Thus the net energy of such a dipole excitation is given by

$$E_{\text{dipole}} = 2(2d-1)V + U - \frac{t_B t_F}{2(2d-1)V} + \frac{dt_B^2}{2(2d-1)V + U} + \frac{dt_F^2}{2(2d-1)V + U}. \quad (40)$$

We note that for $d \gg 1$, where our mean-field theory holds, it is always energetically favorable to create particles and holes well separated since $E_{\text{hopping}}^{B/F} \ll E_{\text{hopping}}^d$. However, the dipolar excitations may become favorable in low dimension and for

large U/V . In this case, $E_{\text{hopping}}^{B/F} \gg E_{\text{hopping}}^d$ for $U \gg V$ and in this limit, the dipolar excitations would be preferred in destabilizing the MI phase. We shall not discuss this issue here any further since this is clearly beyond the scope of our mean-field theory.

Finally, we compute the dispersion of the gapped particle-hole excitations within mean-field theory where the particle and the hole are spatially well separated and do not interact. To this end, we temporarily relax the constraint of conservation of particle number and consider the energy of excitations of adding a particle E_p and a hole E_h to the Mott state. The physical particle-hole excitation energy can then be computed from $E_{ph} = E_p + E_h$. To compute the energy of these particle/hole excitations, we adapt a time-dependent variational approach as done in Ref. 19 for single species Bosons in an optical lattice. We begin with the variational wave function of Bosons and slave bosons (fermions) given by

$$|\psi(t)\rangle = |\psi_B(t)\rangle \times |\psi_F(t)\rangle,$$

$$|\psi_B(t)\rangle = f_0^\alpha(t)|n^B=0\rangle + f_1^\alpha(t)|n^B=1\rangle,$$

$$|\psi_F(t)\rangle = g_0^\alpha(t)|n^a=0\rangle + g_1^\alpha(t)|n^a=1\rangle, \quad (41)$$

where $\alpha=A,B$ denotes sublattice indices. The coefficients f and g satisfy the normalization condition $|f_0|^2 + |f_1|^2 = 1$ and $|g_0|^2 + |g_1|^2 = 1$. We note that at equilibrium $f_0^A = \sin \theta = 0$, $f_1^A = \cos \theta = 1$, $g_0^A = \cos \gamma = 0$, $g_1^A = \sin \gamma = 1$, $f_{0(1)}^B = f_{1(0)}^A$, and $g_{0(1)}^B = g_{1(0)}^A$ for the MI phase.

The Lagrangian of the Bose-Fermi mixture can then be written as

$$\begin{aligned} L' = & \sum_j i[f_{0j}^* \dot{f}_{0j} + f_{1j}^* \dot{f}_{1j} + g_{0j}^* \dot{g}_{0j} + g_{1j}^* \dot{g}_{1j}] \\ & - \sum_{\langle ij \rangle} [-t_B f_{1i}^* f_{0j} f_{0j}^* f_{1j} - t_1 g_{1i}^* g_{0j} g_{0j}^* g_{1j} + V_B |f_{1i}|^2 |f_{1j}|^2 \\ & + V_F |g_{1i}|^2 |g_{1j}|^2] - U \sum_i |f_{1i}|^2 |g_{1i}|^2 + \mu_b \sum_i |f_{1i}|^2 \\ & + \mu_f \sum_i |g_{1i}|^2 - \sum_i \lambda_i (|f_{0i}|^2 + |f_{1i}|^2 - 1) \\ & - \sum_i \nu_i (|g_{0i}|^2 + |g_{1i}|^2 - 1), \quad (42) \end{aligned}$$

where λ_i and ν_i are variational parameters used for implementing the constraint whose values are to be determined from proper choice of the saddle point which in the MI phase yields $\lambda_A = \mu_b$ and $\lambda_B = 0$ for the bosons and $\nu_A = 0$ and $\nu_B = \mu_f$ for the slave bosons.

The saddle-point equations for the variational coefficients $f_i(t)$ and $g_i(t)$ then read

$$i\dot{f}_{0i} + t_B f_{1i} \sum_{\langle j \rangle} f_{1j}^* f_{0j} - \lambda_i f_{0i} = 0,$$

$$i\dot{g}_{0i} + t_1 g_{1i} \sum_{\langle j \rangle} g_{1j}^* g_{0j} - \nu_i g_{0i} = 0,$$

$$\begin{aligned} i\dot{f}_{1i} - & \left[-t_B f_{0i} \sum_{\langle j \rangle} f_{0j}^* f_{1j} + 2V_B f_{1i} \sum_{\langle j \rangle} |f_{1j}|^2 + U f_{1i} |g_{1i}|^2 - \mu_b f_{1i} \right] \\ & - \lambda_i f_{1i} = 0, \end{aligned}$$

$$\begin{aligned} i\dot{g}_{1i} - & \left[-t_1 f_{0i} \sum_{\langle j \rangle} g_{0j}^* g_{1j} + 2V_F g_{1i} \sum_{\langle j \rangle} |g_{1j}|^2 + U g_{1i} |f_{1i}|^2 - \mu_f g_{1i} \right] \\ & - \nu_i g_{1i} = 0. \quad (43) \end{aligned}$$

Next we implement the two-sublattice structure, shift to momentum and frequency space, and expand $f_{ak}^{A/B} = \delta f_{ak}^{A/B} + f_a^{A/B}$ and $g_{ak}^{A/B} = \delta g_{ak}^{A/B} + g_a^{A/B}$, where $a=0,1$. Note that since $\delta f_{ak}^{A/B}$ and $\delta g_{ak}^{A/B}$ correspond to deviation of particle number of the MI state, these dispersions corresponding to their eigenmodes must represent the particle and hole excitations over the MI phase. In the MI phase, we find that the equation of motions for the bosons and the pseudobosons decouple at linear order $\delta f_{ak}^{A/B}$ and $\delta g_{ak}^{A/B}$. For the bosons, we obtain, to linear order in $\delta f_{ak}^{A/B}$,

$$-\omega \delta f_{0\mathbf{k}}^A = -2dt_B c(\mathbf{k}) \delta f_{1\mathbf{k}}^{*B} + \lambda_A \delta f_{0\mathbf{k}}^A,$$

$$\begin{aligned} -\omega \delta f_{1\mathbf{k}}^B = & -2t_B dc(\mathbf{k}) \delta f_{0\mathbf{k}}^A + 2V_B z \delta f_{1\mathbf{k}}^B + U \delta f_{1\mathbf{k}}^B \\ & - (\mu_b - \lambda_B) \delta f_{1\mathbf{k}}^B, \quad (44) \end{aligned}$$

which yields two physical excitation dispersions corresponding to particle and hole excitations

$$\begin{aligned} E_{p(h)} = & + (-) \left(2dV_B + \frac{U}{2} - \mu_b \right) \\ & + \sqrt{\left(2dV_B + \frac{U}{2} \right)^2 - [2t_B dc(\mathbf{k})]^2}. \quad (45) \end{aligned}$$

The energy of a particle-hole excitation which conserves particle number is therefore obtained by adding E_p and E_h and is given by

$$E_{p-h} = 2 \sqrt{\left(2dV_B + \frac{U}{2} \right)^2 - [2t_B dc(\mathbf{k})]^2}. \quad (46)$$

Note that E_{p-h} vanishes along the line $Z = U'/4d$ which agrees with the mean-field result for the SS-MI phase boundary. Also, expanding Eq. (46) to $O(t_B^2)$ for $\mathbf{k}=0$ leads exactly to Eq. (39) which shows that the second-order perturbation theory discussed earlier agrees to the present calculation in the high d limit. Further, at small wave vector, we find $E_{p-h} \sim |\mathbf{k}|$ which shows that the SS-MI quantum phase transition has a dynamical critical exponent $z=1$. Similar dispersion can be obtained for the pseudobosons by considering collective modes corresponding to δg_{ak} . These modes have the same dispersion as Eqs. (45) and (46) with V_B and t_B replaced by V_F and t_1 , respectively.

V. DISCUSSION

Experimental realization of Bose-Fermi mixtures has long been achieved in ultracold atomic systems. These mixtures can be easily tuned to a regime where the on-site intraspecies interaction between both the fermions and the bosons is large

so that they effectively behave as hardcore particles. Thus experimental realization of a Bose-Fermi mixture with $V_B = V_F = 0$ is relatively straightforward. However, most such mixtures do not have sufficiently large nearest-neighbor repulsion and thus it might be difficult to realize mixtures which have large V_F or V_B . Some progress in this direction has recently been made in Ref. 21. Also, use of spin-polarized ^{52}Cr atoms for the fermionic part of the mixture may help since these atoms have significant dipole moment which may provide the requisite interaction.

Once such a Bose-Fermi system is realized, several predictions of the present work can be verified by realizable experiments that are commonly used for ultracold systems. First, we note that since the bosons are spinless and the fermions are spin polarized, the bosonic and the fermionic parts of the mixture can be separated by applying a standard Stern-Gerlach field during a standard time-of-flight experiment as done earlier in Ref. 22 in the context of spinor bosons in optical traps. Such a procedure allows us to separately study the momentum distribution functions of the bosons and the fermions using time-of-flight experiments.¹ For the bosonic cloud, the distinction between the SF and the MI phases can be easily done by measuring the presence or absence of coherence peaks in its momentum distribution as measured in a standard time-of-flight experiment. The precise nature of the broken translational symmetry in the MI and the SS phases for the bosons can also be determined by studying noise correlations of the expanding clouds as already proposed in Ref. 23. Thus, the MI, SS, and SF phases for the bosons can be qualitatively distinguished by these experiments. As for the fermions, the presence/absence of a Fermi surface for the fermions in a trap can be easily distinguished in time-of-flight measurements as performed for ultracold fermions in Ref. 24. Thus, these experiments should allow one to qualitatively distinguish between all four predicted phases. One of the central predictions of our theory is that for any finite U , the metallic state of the fermions shall always be accompanied by a SF phase of the bosons. In terms of time-of-flight experiments this means that any measurement on fermions which sees a gapless Fermi surface shall always be accompanied by corresponding coherence peak (and no density-wave ordering) for the bosons. The collective modes computed in this work can also be verified experimentally using standard inelastic light-scattering experiments.²⁵ Such experiments can detect low-energy collective modes and should thus detect either two (metal+SF phase) or one (SS or

MI+CDW phase) linearly dispersing collective mode(s). The MI phase will be characterized by the absence of any low-energy collective modes of the system.

There are several possible extensions of our analysis. The first and the simplest extension would be to study the phases of the Bose-Fermi mixture away from half filling. This would require a more careful handling of the chemical potential μ_B and μ_F of the bosons and the fermions. In particular one would need to determine t_1 in a self-consistent manner as a function of μ_F . Second, it would be interesting to look at the phase diagram by relaxing the hardcore constraint on the bosons by putting a finite on-site repulsion between them. Of particular interest in this respect is to check if the slave-boson mean field can provide any indication of the phase separation found in such a system in Refs. 14 and 15. Third, it would be useful to study the phase diagram of mixture of spin-polarized fermions with spin-one and spin-two bosons with nearest-neighbor interactions. Such systems are expected to have a much richer phase diagram and have not been theoretically studied so far. Finally, it would clearly be interesting to investigate the effects of quantum fluctuations on the obtained mean-field phase diagram. In the limit $Z = t_B = V_B = V_F = 0$, where our Hamiltonian reduces to the well-known Falicov-Kimball model, we find that the mean-field theory yields qualitatively, but not quantitatively, correct phase diagram and the same holds in the limit of noninteracting fermions where our slave-boson method yields qualitatively similar phase diagram to the DMFT studies of Ref. 15. Inclusion of quantum fluctuations to obtain a quantitatively accurate phase diagram is therefore clearly a possible subject of future study.

To conclude, in this work, we have carried out a slave-boson mean-field analysis of a mixture of hardcore spinless bosons and spin-polarized fermions in an optical lattice. Our analysis provides the mean-field phase diagram of the system and shows the presence of four distinct phases. We have also computed the low-energy collective modes of three of these phases (metal+SF, CDW+MI, and SS) and studied the gapped particle-hole excitation of the fourth (MI). We have discussed experiments which can be used to test our theory and possible extension of our theory to other systems.

ACKNOWLEDGMENTS

We thank Jim Freericks for drawing our attention to the Falicov-Kimball limit of the present model and for several useful discussions.

¹M. Greiner, O. Mandel, T. Esslinger, T. W. Hänsch, and I. Bloch, *Nature (London)* **415**, 39 (2002); C. Orzel, A. K. Tuchman, M. L. Fenselau, M. Yasuda, and M. A. Kasevich, *Science* **291**, 2386 (2001).

²M. P. A. Fisher, P. B. Weichman, G. Grinstein, and D. S. Fisher, *Phys. Rev. B* **40**, 546 (1989); D. Jaksch, C. Bruder, J. I. Cirac, C. W. Gardiner, and P. Zoller, *Phys. Rev. Lett.* **81**, 3108 (1998); K. Sheshadri, H. R. Krishnamurthy, R. Pandit, and T. V. Ra-

makrishnan, *Europhys. Lett.* **22**, 257 (1993).

³D. van Oosten, P. van der Straten, and H. T. C. Stoof, *Phys. Rev. A* **63**, 053601 (2001); K. Sengupta and N. Dupuis, *ibid.* **71**, 033629 (2005).

⁴A. Imambekov, M. Lukin, and E. Demler, *Phys. Rev. A* **68**, 063602 (2003); A. B. Kuklov and B. V. Svistunov, *Phys. Rev. Lett.* **90**, 100401 (2003); A. Kuklov, N. Prokof'ev, and B. Svistunov, *ibid.* **92**, 050402 (2004).

- ⁵L. M. Duan, E. Demler, and M. D. Lukin, *Phys. Rev. Lett.* **91**, 090402 (2003); A. Isacsson, Min-Chul Cha, K. Sengupta, and S. M. Girvin, *Phys. Rev. B* **72**, 184507 (2005).
- ⁶K. Goral, L. Santos, and M. Lewenstein, *Phys. Rev. Lett.* **88**, 170406 (2002); D. L. Kovrizhin, G. Venketeswara Pai, and S. Sinha, *Europhys. Lett.* **72**, 162 (2005); P. Sengupta, L. P. Pryadko, F. Alet, M. Troyer, and G. Schmid, *Phys. Rev. Lett.* **94**, 207202 (2005).
- ⁷M. Greiner, C. A. Regal, and D. S. Jin, *Nature (London)* **426**, 537 (2003).
- ⁸M. W. Zwierlein, J. R. Abo-Shaeer, A. Schirotzek, and W. Ketterle, *Nature (London)* **435**, 1047 (2005); For a review, see R. Onofrio and C. Presilla, *J. Stat. Phys.* **115**, 57 (2004).
- ⁹G. Roati, E. de Mirandes, F. Ferlaino, H. Ott, G. Modugno, and M. Inguscio, *Phys. Rev. Lett.* **92**, 230402 (2004); G. Modugno, E. de Mirandes, F. Ferlaino, H. Ott, G. Roati, and M. Inguscio, *AIP Conf. Proc.* **770**, 197 (2005).
- ¹⁰R. Roth and K. Burnett, *Phys. Rev. A* **69**, 021601(R) (2004); A. Albus, F. Illuminati, and J. Eisert, *ibid.* **68**, 023606 (2003); M. Lewenstein, L. Santos, M. A. Baranov, and H. Fehrmann, *Phys. Rev. Lett.* **92**, 050401 (2004).
- ¹¹M. Cramer, J. Eisert, and F. Illuminati, *Phys. Rev. Lett.* **93**, 190405 (2004); Y. Yu and S. T. Chui, *Phys. Rev. A* **71**, 033608 (2005); F. Illuminati and A. Albus, *Phys. Rev. Lett.* **93**, 090406 (2004); L. D. Carr and M. J. Holland, *Phys. Rev. A* **72**, 031604(R) (2005); K. Sengupta, N. Dupuis, and P. Majumdar, *ibid.* **75**, 063625 (2007).
- ¹²A. Zujev, A. Baldwin, R. T. Scalettar, V. G. Rousseau, P. J. H. Denteneer, and M. Rigol, *Phys. Rev. A* **78**, 033619 (2008); L. Mathey, D.-W. Wang, W. Hofstetter, M. D. Lukin, and E. Demler, *Phys. Rev. Lett.* **93**, 120404 (2004); W. Ning, S. Gu, C. Wu, and H. Lin, *J. Phys.: Condens. Matter* **20**, 235236 (2008); S. K. Adhikari and L. Salasnich, *Phys. Rev. A* **76**, 023612 (2007); M. Rizzi and A. Imambekov, *ibid.* **77**, 023621 (2008); L. Pollet, M. Troyer, K. Van Houcke, and S. M. A. Rombouts, *Phys. Rev. Lett.* **96**, 190402 (2006); A. Imambekov and E. Demler, *Ann. Phys.* **321**, 2390 (2006).
- ¹³L. Mathey, S.-W. Tsai, and A. H. Castro Neto, *Phys. Rev. Lett.* **97**, 030601 (2006); *Phys. Rev. B* **75**, 174516 (2007); F. D. Klonomos and S.-W. Tsai, *Phys. Rev. Lett.* **99**, 100401 (2007).
- ¹⁴H. P. Buchler and G. Blatter, *Phys. Rev. Lett.* **91**, 130404 (2003); *Phys. Rev. A* **69**, 063603 (2004).
- ¹⁵I. Titvinidze, M. Snoek, and W. Hofstetter, *Phys. Rev. Lett.* **100**, 100401 (2008); arXiv:0810.1733 (unpublished).
- ¹⁶Alternatively, we could have chosen the solution $\theta=\pi/2$, $\gamma=0$, and $\Delta\rightarrow-\infty$. This simply amounts to relabeling of *A* and *B* sublattices and corresponds to the same physical state.
- ¹⁷L. M. Falicov and J. C. Kimball, *Phys. Rev. Lett.* **22**, 997 (1969); For a review, see J. K. Freericks and V. Zlatić, *Rev. Mod. Phys.* **75**, 1333 (2003).
- ¹⁸T. Kennedy and E. H. Lieb, *Physica A* **138**, 320 (1986); M. M. Maska, R. Lemanski, J. K. Freericks, and C. J. Williams, *Phys. Rev. Lett.* **101**, 060404 (2008).
- ¹⁹D. Kovrizhin, G. V. Pai, and S. Sinha, arXiv:0707.2937 (unpublished).
- ²⁰J. K. Freericks and H. Monien, *Europhys. Lett.* **26**, 545 (1994); *Phys. Rev. B* **53**, 2691 (1996).
- ²¹C. Ospelkaus, S. Ospelkaus, L. Humbert, P. Ernst, K. Sengstock, and K. Bongs, *Phys. Rev. Lett.* **97**, 120402 (2006).
- ²²J. Stenger, S. Inouye, D. M. Stamper-Kurn, H.-J. Miesner, A. P. Chikkatur, and W. Ketterle, *Nature (London)* **396**, 345 (1998).
- ²³R. H. Brown and R. Q. Twiss, *Nature (London)* **177**, 27 (1956); S. Fölling, G. Gerbier, A. Widera, O. Mandel, T. Gericke, and I. Bloch, *ibid.* **434**, 481 (2005); E. Altman, E. Demler, and M. D. Lukin, *Phys. Rev. A* **70**, 013603 (2004).
- ²⁴M. Kohl, H. Moritz, T. Stoferle, K. Gunter, and T. Esslinger, *Phys. Rev. Lett.* **94**, 080403 (2005).
- ²⁵For a review, see D. Stamper-Kurn and W. Ketterle, arXiv:cond-mat/0005001 (unpublished).